Induction of apoptosis in T lymphoma cells by long-term treatment with thyroxine involves PKCζ nitration by nitric oxide synthase

M. L. Barreiro Arcos, H. A. Sterle, C. Vercelli, E. Valli, M. F. Cayrol, A. J. Klecha, M. A. Paulazo, M. C. Diaz Flaqué, et al.

Apoptosis
An International Journal on Programmed Cell Death

ISSN 1360-8185

Apoptosis
DOI 10.1007/s10495-013-0869-8

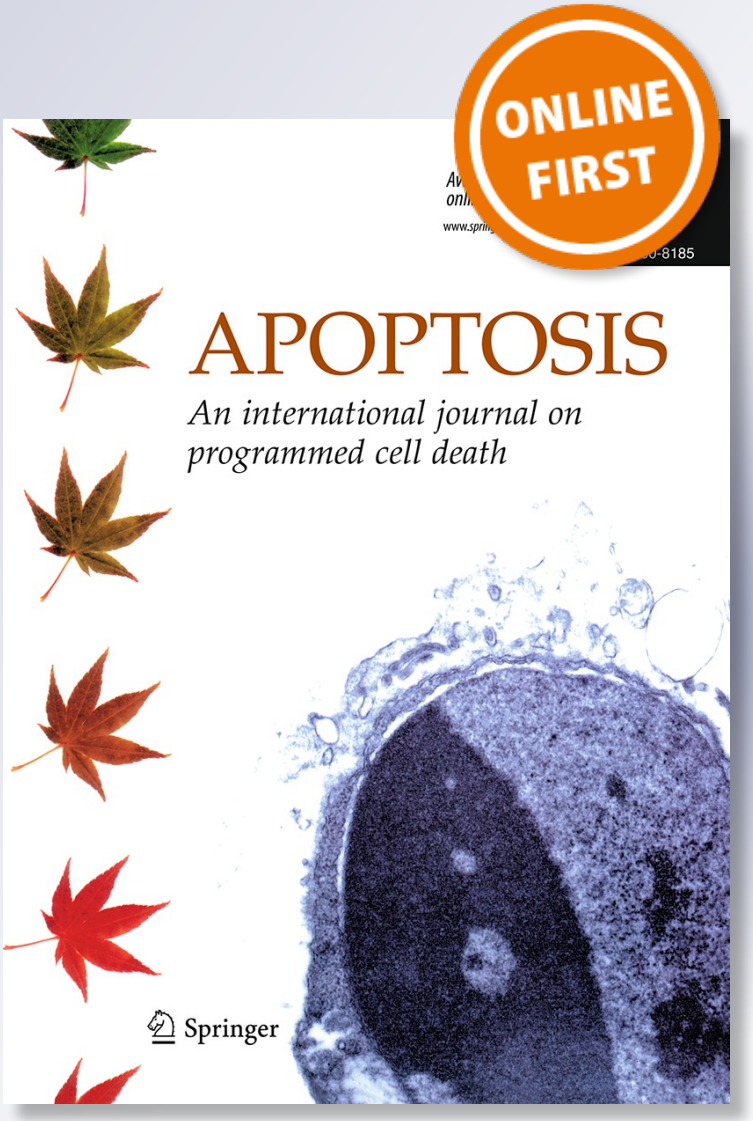

Springer

Apoptosis
DOI 10.1007/s10495-013-0869-8

ORIGINAL PAPER

Induction of apoptosis in T lymphoma cells by long-term treatment with thyroxine involves PKCζ nitration by nitric oxide synthase

M. L. Barreiro Arcos · H. A. Sterle · C. Vercelli · E. Valli · M. F. Cayrol · A. J. Klecha · M. A. Paulazo · M. C. Diaz Flaqué · A. M. Franchi · G. A. Cremaschi

Abstract Thyroid hormones are important regulators of cell physiology, inducing cell proliferation, differentiation or apoptosis, depending on the cell type. Thyroid hormones induce proliferation in short-term T lymphocyte cultures. In this study, we assessed the effect of long-term thyroxine (T4) treatment on the balance of proliferation and apoptosis and the intermediate participants in T lymphoma cells. Treatment with T4 affected this balance from the fifth day of culture, inhibiting proliferation in a time-dependent manner. This effect was associated with apoptosis induction, as characterized through nuclear morphological changes, DNA fragmentation, and Annexin V-FITC/Propidium Iodide co-staining. In addition, increased iNOS gene and protein levels, and enzyme activity were observed. The generation of reactive oxygen species, depolarization of the mitochondrial membrane, and a reduction in glutathione levels were also observed. The imbalance between oxidants and antioxidants species is typically associated with the nitration of proteins, including PKCζ, an isoenzyme essential for lymphoma cell division and survival. Consistently, evidence of PKCζ nitration via proteasome degradation was also observed in this study. Taken together, these results suggest that the long-term culture of T lymphoma cells with T4 induces apoptosis through the increased production of oxidative species resulting from both augmented iNOS activity and the loss of mitochondrial function. These species induce the nitration of proteins involved in cell viability, promoting proteasome degradation. Furthermore, we discuss the impact of these results on the modulation of T lymphoma growth and the thyroid status in vivo.

Keywords Thyroid hormones · T lymphoma · Apoptosis · Oxidative stress · Nitric oxide synthase · Protein kinase C · Protein tyrosine nitration

M. L. Barreiro Arcos · H. A. Sterle · E. Valli · M. F. Cayrol · A. J. Klecha · M. A. Paulazo · M. C. Diaz Flaqué · G. A. Cremaschi (✉)
Instituto de Investigaciones Biomédicas, Facultad de Ciencias Médicas, Pontificia Universidad Católica Argentina (UCA), CONICET, Alicia M. de Justo 1600 3° piso, CABA, Buenos Aires, Argentina
e-mail: gacremaschi@yahoo.com

C. Vercelli
Instituto de Investigación en Biomedicina de Buenos Aires (CONICET), Buenos Aires, Argentina

A. J. Klecha · G. A. Cremaschi
Laboratorio de Radioisótopos, Facultad de Farmacia y Bioquímica, Universidad de Buenos Aires, Buenos Aires, Argentina

A. M. Franchi
Centro de Estudios Farmacológicos y Botánicos (CEFYBO), CONICET, Facultad de Medicina, Universidad de Buenos Aires, Buenos Aires, Argentina

Introduction

Thyroid hormones (THs), 3,5,3′-L-triiodothyronine (T3) and thyroxine (T4), exert profound effects on metabolism, growth, and development, affecting almost all tissues. At the cellular level, both T3 and T4 influence proliferation, differentiation and apoptosis in different cell types [1–3]. Most of these actions are mediated through thyroid hormone nuclear receptors (TRs), which are widely expressed in mammalian tissues. Both T3 and T4 act via TRs, but the affinity of the receptor for T4 is much lower than that for T3. Thus, T3 is the natural ligand of TRs. In the genomic

Published online: 04 June 2013

concept of hormone action, T4 is considered as a prohormone converted to the more metabolically active T3 through tissue deiodinase. In addition, T4 initiates rapid nongenomic mechanisms at the cell membrane through the mediation of signal transduction pathways. Nongenomic and genomic mechanisms of TH action interface in the cell nucleus, as TH extranuclear activation of intracellular signaling pathways alter the transcriptional activity of nuclear hormone receptors [4, 5].

TH-mediated effects on proliferation and apoptosis depend on the type and developmental or pathophysiological state of the cell/tissue. The clearest example of TH action in the regulation of cell physiology is amphibian metamorphosis, which is strictly controlled through T3. The striking stages in this process include the complete involution, remodeling, and development of some organs. The T3-mediated induction of both apoptosis and cell proliferation is responsible for the changes observed in these stages [6, 7]. THs are also considered primary mitogens for hepatocytes [1] and play a role in the proliferation of keratinocytes and epidermal cells [8], cardiomyocytes [9], pancreatic acinar [10, 11] and thyroid cells [12]. In contrast, THs also block cell proliferation and induce the differentiation of N2a-β neuroblastoma cells [13]. THs also inhibit proliferation and stimulate the functional maturation of Sertoli cells in prepubertal rat testis through increased levels of cyclin-dependent kinase inhibitors [14]. Moreover, the TH-mediated inhibition of proliferation was also demonstrated in mammary epithelial cells [15].

Apoptosis induced mechanisms were also demonstrated in different cell types, such as rat pituitary cell lines [16, 17] and human breast cancer cells [18], when exposed to THs. Consistently, in HeLa and rat thyroid cells overexpressing TRs, T3 induces caspase activity, which plays a key role in the execution of apoptosis [19]. However, the physiological concentrations of both T3 and T4 inhibit apoptosis in rat brain-derived endothelial cells in vitro through alterations in the mRNA levels of Bcl2 and Bad, two apoptosis-related genes [20]. Moreover, T4 modulates resveratrol-induced apoptosis in glioma cells through nongenomic mechanisms [21].

The actions of THs are not clearly defined at lymphocyte level. Few reports analyzing the in vitro actions of THs show alterations in lymphocyte reactivity. However, the direction and magnitude of these alterations might depend on the type and concentration of the TH encountered by the responding cells, and the species source of lymphoid cells [22–24]. However, the precise physiological mechanisms underlying TH effects have not been studied. Recently, we characterized the direct actions of THs on T lymphocyte proliferation. After 24 to 72 h of treatment, THs stimulate or induce the proliferation of normal and tumor T cells, respectively [25]. Furthermore, in BW5147 (BW) T lymphoma cells these actions are mediated through the activation of the inducible isoform of nitric oxide synthase (iNOS), stimulated through the atypical ζ isoenzyme of protein kinase C (PKC), a crucial enzyme for BW cell growth [26]. Moreover, the participation of TH-mediated nongenomic mechanisms in BW cell proliferation has been demonstrated, and the signaling cascade involves sphingomyelinases acting up-stream of PKCζ activation, and ERK and NF-κB activation downstream of this PKC isoenzyme. These mechanisms increase the expression of TRα_1 at both the protein and mRNA levels, but the increase in iNOS gene expression and activity was associated with the binding of T3 to its nuclear receptor [27].

Nevertheless, T lymphocytes apoptosis occurred after THs exposure. Indeed, Mihara et al. [28] demonstrated that T lymphoma cells from the human Jurkat cell line, cultured in vitro for 2 weeks with T3 and T4, but not TSH or TRH, showed enhanced apoptosis. These authors also showed that T lymphocytes from healthy volunteers cultured with T3, but not T4, for 5 days displayed an increase in the percent of spontaneous apoptosis. Similar findings were observed when peripheral blood T lymphocytes from patients with Graves' disease, the most common cause of hyperthyroidism, were cultured for 24 h, thus indicating that chronic exposure to THs induces accelerated lymphocyte apoptosis both in vivo and in vitro. However, the association of T3 with the reduced incidence of lymphocyte apoptosis was also shown under normal physiological conditions in healthy older individuals [29].

Thus, the aim of this study was to characterize the action of THs on BW cells under long-term culture conditions and unravel the biochemical and molecular mechanisms involved in these effects. These findings will improve the knowledge of TH-mediated regulation of lymphocyte physiology and clarify the putative and controversial participation of THs in neoplasia-dependent mechanisms.

Materials and methods

Cell suspensions and culture conditions

The tumor cell line BW5147.3 (American Type Culture Collection (ATCC), Catalog Number TIB-47) is a mouse T cell lymphoma that expresses H-2^k haplotype, CD3$^+$, and the αβ T-cell receptor, confirmed through flow cytometry with specific antibodies against the corresponding surface markers [27]. These cells were cultured at an optimal concentration of 1–5 × 10^5 cells/ml in RPMI 1640 medium (GIBCO BRL) supplemented with 10 % fetal calf serum (FCS), 2 mM glutamine, and antibiotics, with twice weekly splitting after reaching exponential growth.

Proliferation assays

Cells cultured at concentration of 0.5×10^6 cells/ml were settled at a final volume of 0.2 ml in 96-well flat-bottom microtiter plates (Nunc) and pulsed with [^{3}H]thymidine ([^{3}H]TdR, NEN, 20 Ci/mmol) for the last 6 h of incubation, as previously described [27]. The results are expressed as dpm values in experimental cultures, subtracting the dpm control values obtained in the absence of T4.

Chromatin condensation assay

T lymphoma cells were cultured in RPMI 1640 medium supplemented with FBS in the absence or presence of T4 for the times indicated, and the nuclear morphology was examined. Briefly, the cells were washed and resuspended in PBS at a concentration of 1×10^6 cells/ml, plated onto slides and fixed with ethanol. Nuclear staining solution containing 0.01 mg/ml Hoechst 33342 was added for 10 min. The cells were washed three times with PBS, and the nuclei were subsequently examined using a fluorescent microscope (Nikon Diaphou; Nikon Inc., Melville, NY).

DNA fragmentation analysis using agarose gel electrophoresis

Inter-nucleosomal DNA fragmentation was analyzed in BW T cells according to the methods of Herrmann et al. [30]. Briefly, after harvesting, the samples from cultures with or without THs were washed with PBS and pelleted through centrifugation at $1{,}200\times g$ for 10 min. The cell pellets were subsequently treated for 10 s with lysis buffer (1 % Igepal in 20 mM EDTA and 50 mM Tris–HCl, pH 7.5) and after centrifugation for 5 min at $1{,}600\times g$ the supernatant was collected. The supernatants were treated with 1 % SDS and RNase A for 2 h (final concentration 5 μg/μl) at 56 °C, followed by digestion with proteinase K (final concentration 2.5 μg/μl) for at least 2 h at 37 °C. After the addition of 5 M ammonium acetate, the DNA was precipitated with 2.5 volumes of ethanol and separated on a 2 % agarose gel. The DNA was visualized and photographed under UV light after ethidium bromide (0.5 μg/ml) staining.

Quantification of apoptosis using flow cytometry

BW cells were incubated in the absence or presence of T4 for the indicated times. Subsequently, 1×10^6 cells were washed once with PBS, resuspended in staining buffer (10 mM HEPES/NaOH, pH 7.5; 0.14 M NaCl; 2.5 mM $CaCl_2$) and incubated for 15 min in the dark with 5 μl of Annexin V-FITC (1 mg/ml, SIGMA Chemical Co.) and 10 μl of propidium iodide (PI, 1 mg/ml SIGMA Chemical Co). Labeled cells were analyzed through flow cytometry (FACSCalibur, Becton Dickinson Biosciences), quantifying the fluorescence intensity at 580 (PI) and 520 nm (Annexin V-FITC). The data were analyzed using WinMDi 2.8 software and expressed as the percentage of cells in each condition (Annexin and PI negative, Annexin positive PI negative, Annexin and PI positive) with respect to the total cells analyzed [31].

Nitric oxide synthase activity determination

Nitric oxide synthase activity was measured through the production of [U-^{14}C]citrulline from [U-^{14}C]arginine (Amersham Biosciences) [25, 26]. The specificity of NOS activity was evaluated in the presence of the NOS blocker, NG-monomethyl-L-arginine monoacetate (L-NAME). Briefly, 1×10^6 cells were incubated in 500 μl Krebs buffer, in the presence of [^{14}C]-arginine (0.5 μ Ci) for 30 min. To ensure the conversion of [U-^{14}C]-arginine to [U-^{14}C]-citrulline via NOS, L-valine, an inhibitor of the alternative arginase pathway of $^{\bullet}$NO production, was added during the incubation with radiolabeled arginine. After incubation, the cells were disrupted through sonication (Vibra-cell, Sonics and Materials) in a medium containing 10 mM EGTA, 0.1 mM citrulline, 0.1 mM dithiothreitol, and 20 mM Hepes, pH 7.5. After centrifugation at $20{,}000\times g$ for 10 min, the supernatants were applied to 2 ml columns of Dowex AG 50WX-8 (sodium form, Bio-Rad), and the [U-^{14}C]-citrulline was eluted with 3 ml of water and quantified through liquid scintillation counting.

Determination of nitrite concentrations

To assess the amount of $^{\bullet}$NO produced, nitrite, the stable end product of $^{\bullet}$NO in solution, was measured using a colorimetric assay based on the Griess reaction [26]. Briefly, 1×10^6 cells/ml were cultured in supplemented RPMI medium without phenol red in 24-well plates under basal conditions or in the presence of T4 for the indicated times. The cultures were also incubated in the presence of the NOS blocker L-NAME for the last 6 h of culture to ensure that nitrite production depended on NOS activity. Nitrite production was evaluated in the supernatants during the last 24 h of culture. One hundred microliters of supernatant was dispensed in 96-well microplates, followed by the addition of 100 μl of a reactive solution containing 1 % sulfanilamide with 0.1 % *N*-(1-naphthyl) ethylenediamine dihydrochloride with 25 % HCl (0.4 M final concentration). The standard calibration curve was constructed using known concentrations of sodium nitrite. The optical densities were measured at 540 nm using an ELISA plate reader (Uniskan Labsystem).

Immunoblot analysis

Lymphoma T cells (5×10^6) were lysed for 30 min at 4 °C in lysis buffer (50 mmol/l Tris–HCl, 150 mmol/l NaCl, 1 mmol/l EGTA, 1 % Igepal, 1 mmol/l NaF, 1 mmol/l Na_3VO_4, 0.25 % sodium deoxycholate, 1 μmol/l phenylmethylsulfonyl fluoride, 19 μg/ml aprotinin, 10 μmol/l pepstatin and 10 μmol/l leupeptin). After centrifugation (14,000×*g*, 15 min, 4 °C), the whole-cell protein extracts (50 μg) were mixed with SDS-sample buffer (2 % SDS, 10 % (v/v) glycerol, 62.5 mM Tris–HCl, pH 6.8, 0.2 % bromophenol blue and 1 % (v/v) 2-mercaptoethanol). Equal amounts of proteins were separated through SDS-PAGE on 10 % polyacrylamide gels and transferred to PVDF membranes. Nonspecific binding sites on the PVDF membranes were blocked using blocking buffer (5 % nonfat dried milk containing 0.1 % Tween 20 in 100 mM Tris–HCl, pH 7.5 and 0.9 % NaCl) for 1 h. Subsequently, the PVDF membranes were incubated overnight with rabbit anti-PKCζ, mouse anti-iNOS (both obtained from SIGMA Chemical Co.), rabbit anti-nitrotyrosine (Santa Cruz Biotechnology, Inc.), rabbit anti-active caspase 9, rabbit anti-active caspase 3 (both of Abcam, MA, USA) or mouse anti-cleaved PARP (BD Biosciences, NJ, USA) antibodies. All antibodies were used at a dilution of 1:1,000, except for the anti-nitrotyrosine antibody, which was used at a 1:200 dilution. After washing three times for 10 min with PBS-Tween, the membranes were sequentially exposed to anti-mouse (1:2,000) or anti-rabbit (1:5,000) antibodies coupled to horseradish peroxidase (Amersham Pharmacia Biotech) for 1 h. After the membranes were washed three times for 10 min with PBS-Tween and once with PBS, an enhanced chemiluminescent system (Amersham Pharmacia Biotech) was used for detection. The amount of protein loaded in each well was determined using a rabbit polyclonal anti-β-actin antibody (1:1,000, Sigma Chemical Co.). The densitometry analysis of the bands was performed using Image J software (version 5.1, Silk Scientific Corporation, NIH, Bethesda, MA, USA). The densitometry intensities of the analyzed proteins were normalized to those of the corresponding bands for β-actin.

Total RNA extraction

Total RNA was extracted from BW cells (3×10^6) incubated or not in the presence of T4 (1×10^{-7} M) using 1 ml Tri-reagent (Genbiotech SRL) per sample. After 5 min incubation at room temperature, 200 μl of chloroform was added to the tubes and centrifuged at 12,000×*g*. The aqueous phase was transferred to another tube and the RNA was pelleted through centrifugation (12,000×*g*) with cold ethanol and dried in air. The RNA pellets were dissolved in RNase-free water and stored at −70 °C. To quantify the RNA concentration, the absorbance at 260 nm was measured (Nanodrop ND-1000, UK). The purity of the RNA preparations was assessed using spectrophotometry at a 260/280 nm ratio and 1 % agarose gel stained with ethidium bromide. The samples were used for RT-PCR analysis.

Reverse transcription (RT)-polymerase chain reaction (PCR) and real-time quantitative PCR (qPCR)

Total RNA (2 μg) was used for the synthesis of cDNA using the Omniscript kit (Qiagen). Briefly, the cDNA was synthesized using 1 μM of oligodeoxythymidine$_{12–18}$ (Biodynamics SRL) in a 20 μl reaction containing 5 mM of each dNTP, four units of Omniscript Reverse Transcriptase and 2 μl 10× buffer RT (provided by the kit) at 37 °C for 1 h according to the manufacturer's instructions.

The PCR reaction was performed in a total volume of 25 μl, containing 25 mM $MgCl_2$, 10 pmol of the primers, 25 mM of each nucleotide (dATP, dCTP, dGTP and dTTP, Promega), 1.5 U of Taq DNA polymerase (Promega) and 2 μl of cDNA (2.5 μg). The PCR reactions were performed in a DNA thermal cycler (Progene, Techne). The primers (Biodynamics SRL) used in the current study were designed to amplify a 262-bp band for iNOS mRNAs, a 207-bp band for PKCζ isoform and a 300-bp band for β2-microglobulin (housekeeping gene).

The primers sequences, which are shown in Table 1, were designed using Primer Express software version 3.0 (Applied Biosystems). The cycling conditions were 95 °C for 5 min, followed by 32 cycles of 95° for 1 min, 62 °C for 1 min for iNOS and β2-microglobulin, 62 °C for 1 min for PKCζ and 72 °C for 1 min, with a final extension at 72 °C for 10 min. The PCR products were run on a 2 % agarose gel and stained with ethidium bromide [25, 27].

In addition, qPCR was performed in a Rotor Gene 6000 and mRNA levels were quantified using SYBR Green technology (Biodynamics SRL). The target gene expression was quantified using the comparative cycle threshold (C_t) method according to the manufacturer's instructions (Applied Biosystems). An average C_t was calculated from the duplicate reactions and normalized to β2-microglobulin.

Reactive oxygen species measurement

Reactive oxygen species generation was assessed using 2,7 dichlorofluorescein diacetate (DCFH-DA) and hydroethidine (HE). Initially, neither of these chemicals are fluorescent probes; however, upon oxidation through ROS, both substances are converted to highly fluorescent derivatives. Briefly, 1×10^6 BW cells were resuspended in 1 ml phosphate-buffered saline (PBS) and incubated with

Table 1 Primer sequences used for real time RT-PCR. The primers were designed using mouse cDNA sequences available in the UniGene database according to the criteria of the Primer Express software (Applied Biosystems)

Gene	Primers sequences
iNOS	5′-TCAGACATGGCTTGCCCCTGGA-3′ (forward) 5′-TGCCCCAGTTTTTGATCCTCACA-3′ (reverse)
PKCζ	5′-CGATGGGGTGGATGGGATCAAAA-3′ (forward) 5′-AACACATGTTTCTCTGTCTG-3′(reverse)
β2-microglobulin	5′-GCTATCCAGAAAACCCCTCAA-3′ (forward) 5′-CATGTCTCGATCCCAGTAGACGGT-3′ (reverse)

20 μM DCFH-DA or 10 μM HE for 20 min at 37 °C. DCFH-DA and HE fluorescent products were measured using a flow cytometer (FACSCalibur, Becton Dickinson Biosciences) at 488 nm. The data were analyzed using WinMDi 2.8 software.

Determination of total glutathione and glutathione disulfide levels

BW cells were cultured in the absence or presence of T4 for the indicated times. Subsequently, the cells were washed, resuspended in PBS and pelleted at 1,000×*g* for 10 min. The cell pellets were resuspended in 200 μl of 0.5 % TCA and frozen at −20 °C. The pellets were thawed and centrifuged to remove the cellular debris. The supernatants were used to quantify total glutathione (the tripeptide γ-glutamyl-cysteinyl-glycine) and GSSG levels. The glutathione levels were determined using the method of Griffith [32]. The total glutathione was evaluated using the enzyme recycling procedure, in which glutathione is oxidized through 5, 5′-dithiobis-2-nitrobenzoic (DTNB) acid and reduced through NADPH in the presence of glutathione reductase. 2-Nitro-5-thiobenzoic acid (TNB) formation was monitored at 412 nm. The total glutathione values in the sample were extrapolated to a standard curve of known concentrations of the tripeptide. For GSSG quantification, the samples were preincubated with 4-vinylpyridine (an inhibitor of DNTB mediated oxidation). Reduced glutathione (GSH) was determined after subtracting the GSSG values from the total glutathione [32].

Determination of mitochondrial membrane potential

The cells were cultured with T4 for the indicated times, and aliquots of the cell cultures (1×10^6 cells/ml) were incubated with 1 μM Rhodamine-123 (Rho-123; Sigma Chemical Co.) for 30 min. Subsequently, the cells were centrifuged and resuspended in PBS and the fluorescence was quantified using a FACSCalibur flow cytometer. Rho-123 is a cell-permeant, cationic, green-fluorescent dye ($\lambda_{ex/em}$ 505/560 nm), which selectively accumulates on the inside of the mitochondria. When the mitochondrial membrane potential is damaged, the dye is not retained in the mitochondria and a reduction in the fluorescence intensity is detected through flow cytometry.

PKC immunoprecipitation

For the total protein extraction, BW cells were washed twice in PBS and centrifuged at 3,000×*g* for 10 min. The pellet was subsequently lysed in ice-cold lysis solution (140 mM NaCl, 10 mM Tris HCl, 1 mM EDTA, 5 mM NaF, 1 % Triton X-100, 2 μg/ml aprotinin, 10 μg/ml leupeptin, 10 μg/ml DTT, 100 μg/ml soybean trypsin inhibitor and 1 mg/ml benzamidine, pH 7.4). The homogenates were sonicated for 30 s and incubated for 1 h at 4° C with agitation. The homogenates were further centrifuged at 10,000×*g* for 5 min to remove the nuclei and organelles. An aliquot of the cell suspension was analyzed through SDS-PAGE (total fraction). The protein content was determined using the Bradford Bio-Rad protein assay (Bio-Rad). For the co-immunoprecipitation assays, 125 μg of total lysate protein was incubated with 2 μg of anti-PKCζ antibody in a final volume of 50 μl of immunoprecipitation buffer (1 % Igepal, 10 % glycerol, 10 mM HEPES and 150 mM NaCl and protease inhibitors, pH 7.8) overnight at 4 °C, and subsequently, 20 μl of Protein A/G-Sepharose beads (Plus-Agarose, Santa Cruz, Biotechnology Inc.) was added for 4 h at 4 °C. The mixture was centrifuged at 7,000×*g* for 2 min, and the supernatant was separated from the pellet. The protein concentration in both fractions was determined using the Bradford assay. Finally, the samples were boiled in sample buffer, and the bands were revealed using specific antibodies anti-PKCζ and anti-DNP-groups through SDS-PAGE.

Statistical analysis

Student's *t* test for unpaired values was used to determine the levels of significance. When multiple comparisons were necessary after analysis of variance, the Student–Newman–Keuls test was applied. Differences between the means were considered significant if $P \leq 0.05$.

Results

Inhibition of T lymphocyte proliferation after long-term treatment with T4

We previously showed that THs induce the proliferation of murine T lymphoma BW cells when incubated for 24–72 h [25, 27]. As T4 is the most widely used hormone in hypothyroidism therapy, the possibility that T4 also induces apoptosis during longer treatments was also evaluated. The incubation of BW cells in the presence of T4 (10^{-7} M) for 5 or more days inhibited cell growth (Fig. 1a). In addition, the cells showed nuclear morphology compatible with apoptosis, such as the reduction of the nucleus and cytoplasm volume, chromatin condensation and apoptotic corpus formation (Fig. 1b), thus indicating that cells undergo apoptosis. These effects were more pronounced with increasing culturing time in the presence of T4, which was evident at 7 days and reached the maximum level of chromatin condensation at 15 days (Fig. 1b). The induction of apoptosis was confirmed using the DNA ladder technique, as cells incubated with T4 for 5 days or more displayed DNA degradation characteristic of endonuclease action. Figure 1c shows the gradient of fragmented DNA.

The percentage of viable and necrotic cells, and cells at different stages of apoptosis was quantified through Annexin V-FITC and propidium iodide staining, followed by flow cytometry. Figure 1d shows that treatment with T4 increases the number of apoptotic cells in a time-dependent manner. Notably, BW cells growing under basal conditions (cells in exponential growth and cells not treated with hormone) showed 97 ± 2 % viability (Annexin-/IP-), independent of the cell sampling time. T4 treatment for 5 or more days reduced cell viability and increased the percentage of cells in the early and late stages of apoptosis as a function of time. At day 15 of incubation with T4, 96 ± 2 % of cells were in late apoptosis with a number of viable cells below 1 %. In addition, physiological concentrations of T3 and T4 (1 nM) similarly affected cell viability, but T3 showed greater variation (data not shown); thus, the mechanisms involved in the induction of TH-mediated apoptosis in BW cells were further studied using T4.

Regulation of NOS levels

We previously described that THs increase the production of •NO in BW cells after 24–48 h of incubation. This increase was mediated through an increment in the activity and expression of iNOS and is associated with T4-mediated BW cell proliferation; notably, this effect was abrogated using NOS and iNOS inhibitors [25, 27]. To determine whether iNOS was also involved in the mechanisms underlying apoptosis through long-term treatment with T4, both NOS enzymatic activity and iNOS protein and gene expression were analyzed. As shown in Fig. 2a, NOS enzymatic activity was markedly increased between 5 and 10 days of incubation in the presence of T4, which was significantly greater than that induced at 48 h (150 ± 8 pmol/10^7 cells). Similar results were observed when nitrite production was assessed (Fig. 2b). Notably, NOS activity and nitrite production were determined in the presence of L-Valine (50 mM), an inhibitor of arginases, to rule out the conversion of arginine through arginases. With incubation times longer than 10 days, both NOS activity and nitrite production were reduced, and a significant loss of viable cells was also observed. Indeed, at 21 days of incubation, when the percentage of viable cells is lower than 1 %, •NO levels reached values below that of the control. The reduction in NOS activity was associated with a change in the protein and gene expression of the NOS inducible isoform. As shown in Fig. 2c and d, T4 incubation for 5 days increased the levels of iNOS protein, which remained high until 10 days of culture, diminishing after 15 days when the loss of cell viability reached a maximum value. The conventional and real-time PCR analysis indicated that T4 increased the mRNA expression of iNOS, reaching a maximum value after 3 days of incubation (Fig. 2e, f). As expected, the increase in mRNA expression was prior to the increase in its protein levels.

Fig. 1 Effect of long-term T4 treatment on BW cell proliferation and viability. **a** Quantification of BW T lymphoma cell proliferation. The cells (1×10^6 cell/ml) were cultured at exponential growth in the absence (*dotted lines*) or presence of T4 (10^{-7} M, *continuous lines*) for the indicated times. Proliferation was evaluated using a 6-h pulse of [^{3}H]TdR. The results are presented as the mean ± SE of 3 independent experiments performed in triplicate. * Differ significantly from the corresponding basal with $P < 0.01$. **b** Nuclear morphology of cells incubated in the absence (Basal) or the presence of T4 (10^{-7} M) for the indicated times, followed by staining with Hoechst 33342. The fluorescence microscopy images are representative of 4 independent assays at ×1,000 magnification. **c** DNA ladder analysis of BW cells cultured in the absence (Basal) or presence of T4 (10^{-7} M) for the indicated times. The agarose gel electrophoresis image is representative of 3 independent experiments. **d** Evaluation of cellular apoptosis using Annexin-FITC/PI staining, followed by flow cytometry. The BW cells were incubated in the absence (Basal, untreated exponential cells sampled at day 5) or presence of T4 (10^{-7} M) for the indicated times, followed by staining with Annexin V-FITC and PI. Notably, the basal values for 7 and 15 days were 97.3 ± 1.5 and 96.8 ± 2.0, respectively. The percentages of viable cells (Annexin V-FITC −/PI−), and those showing early apoptosis (Annexin V-FITC +/PI−), late apoptosis or necrosis (Annexin V-FITC +/PI +) and only necrosis (Annexin V-FITC −/PI+) with respect to the total number of cells are shown in the dot blot graphics. The results are representative of 4 independent assays. The bar graph shows the mean ± SE of the percentage of cells corresponding to each stage. * Significantly different from the corresponding basal values ($P < 0.05$)

Increase in oxidative stress

To examine the possibility that the increase in NOS activity mediated through T4 would be accompanied with the

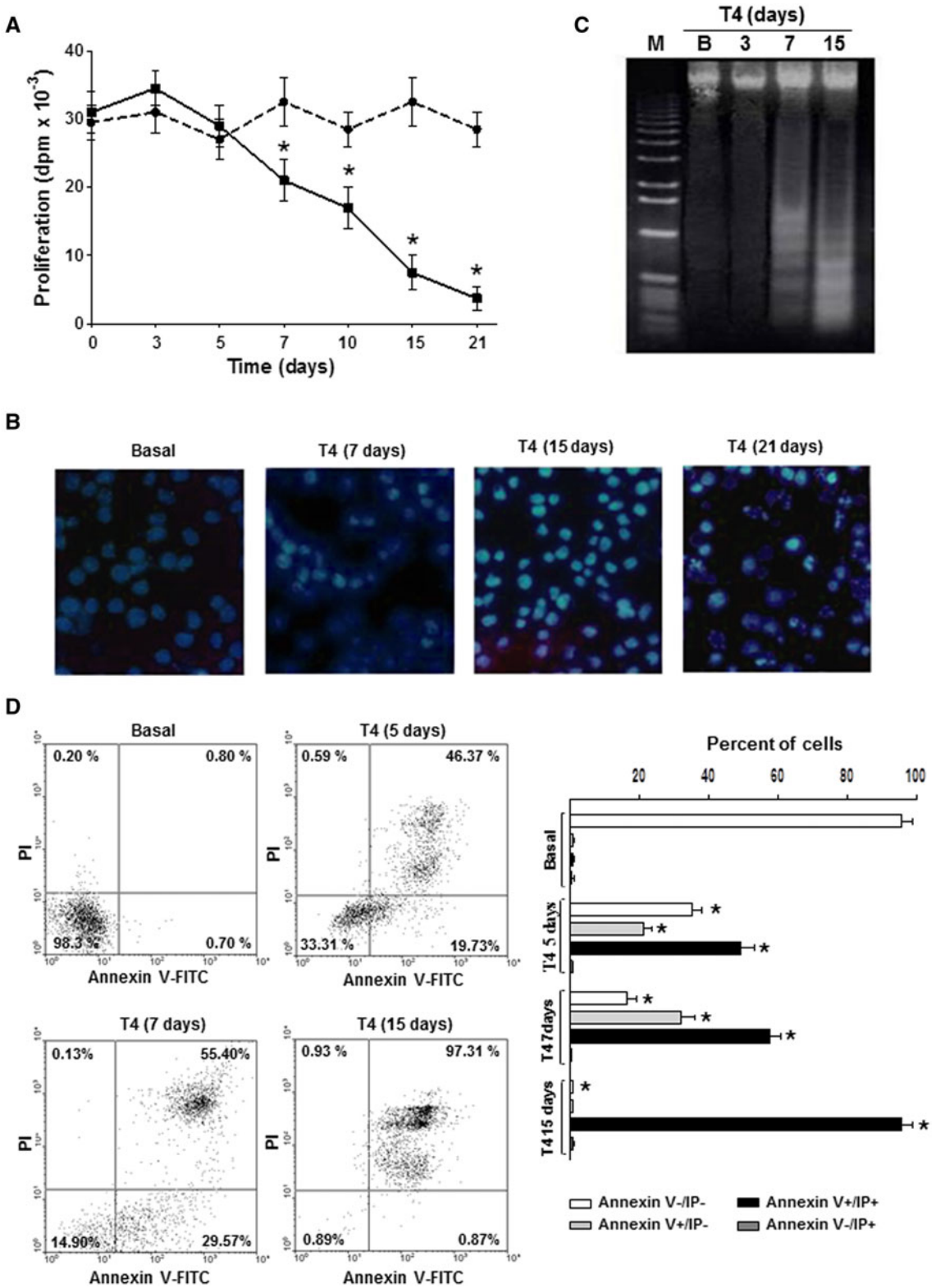

accumulation of reactive oxygen species (ROS), DCFH-DA and DHE oxidation were used to detect ROS levels using flow cytometry (Fig. 3a, b). Long-term treatment with T4 increased the ROS content and correlated with a loss in cell viability. To analyze whether the increase in oxidizing molecules alters the content of antioxidant

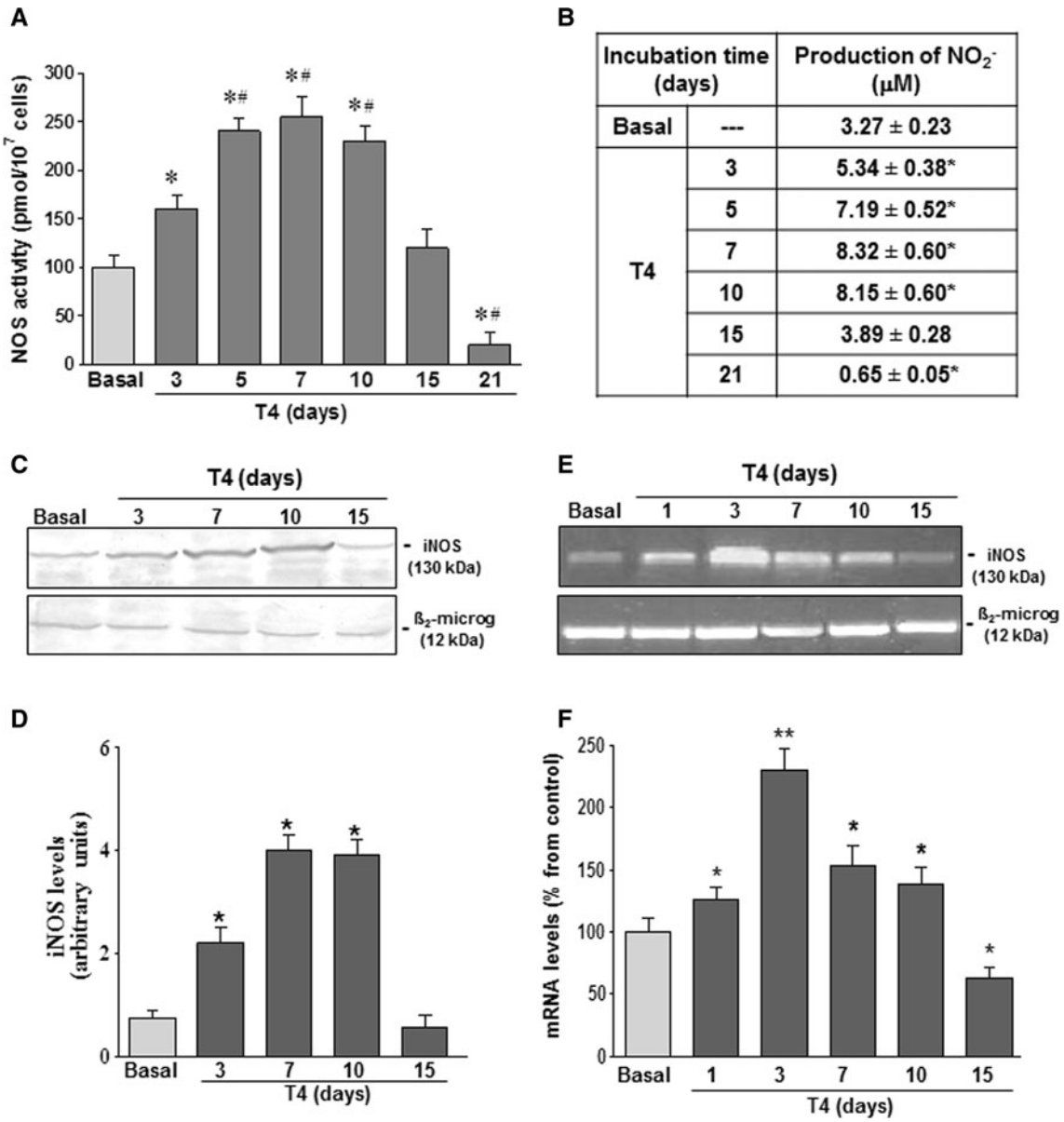

Fig. 2 Long-term T4 actions on NOS activity and expression. BW cells (1–2 × 10^6 cells/ml) were incubated in the absence (Basal) or the presence of T4 (10^{-7} M) for the indicated times. NOS activity was measured through the enzymatic conversion of [^{14}C]-arginine to [^{14}C]-citrulline (**a**) and nitrite production using the Griess method (**b**). The values represent the mean ± SE of 3 experiments performed in triplicate. The analysis iNOS protein expression was determined through western blot analysis (**c**), and the iNOS mRNA expression was examined using conventional (**d**) and qRT-PCR (**e**) methods. The results are representative of 4 independent experiments. For the mRNA quantification, the results represent the mean ± SE of 3 experiments. Differ significantly from the corresponding basal values, with * $P < 0.01$ or ** $P < 0.001$

species, the balance between reduced and total glutathione levels was evaluated. As shown in Fig. 3c, long-term T4 treatment decreased the content of reduced glutathione, without altering total glutathione levels, and diminished the GSH/GSSG ratio (Fig. 3d). This imbalance between the intracellular levels of oxidants and antioxidants species could contribute to T4-mediated apoptosis.

Mitochondria depolarization in ROS generation

To examine the possibility that the mitochondrial membrane depolarization plays a role in the cascade of intracellular signals for the induction of cell apoptosis, changes in mitochondrial membrane potential were evaluated using Rhodamine-123 staining on cells cultured in the absence or

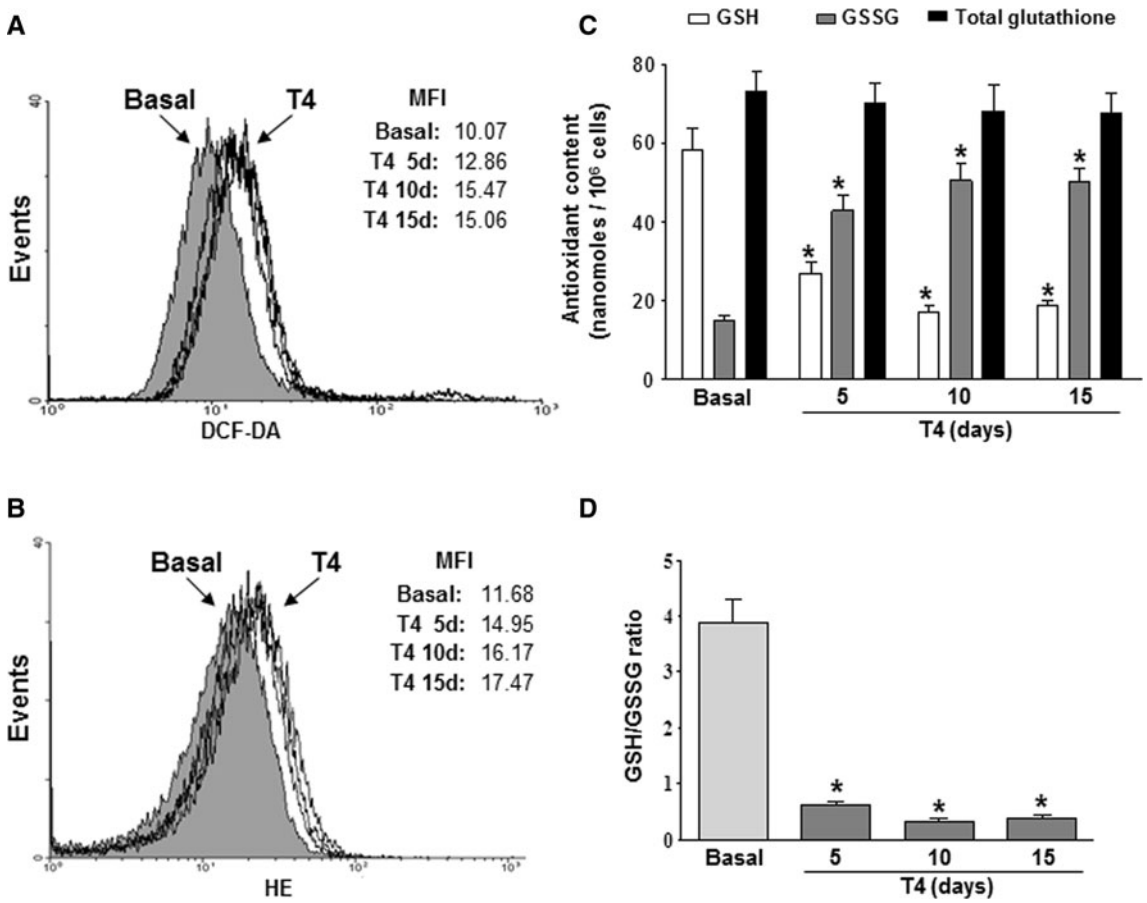

Fig. 3 Production of oxidizing species and modulation of antioxidants molecules by long-term treatment with T4. BW cells were incubated in the absence (Basal) or the presence of T4 (10^{-7} M) for the indicated times and labeled with DCFH-DA (**a**) or HE (**b**) to evaluate the production of oxidizing species through flow cytometry. The histograms are representative of 3 independent experiments performed in duplicate. The mean fluorescence intensity (MFI) of each curve is also displayed. GSH, GSSG and total glutathione were quantified as indicated in the "Materials and methods" (**c**). GSH/GSSG ratio is shown in **d**. The values represent the mean ± SE of 3 experiments performed in triplicate. * Differ significantly from the corresponding basal values, with $P < 0.001$

presence of T4 for more than 5 days. As shown in Fig. 4(a, b), the long-term treatment of BW cells with T4 reduced the mitochondrial membrane potential. These results indicate that T4 might induce intrinsic apoptosis through mitochondria depolarization.

Effects of T4 on caspase proteolytic activation and PARP cleavage

To analyze the participation of the intrinsic mitochondrial pathway in the induction of apoptosis mediated through T4, we performed a western blot analysis of the protein levels of active caspase 9. As shown in Fig. 5, the long-term incubation of BW cells with T4 induced the proteolytic activation of caspase 9. In addition, an increase in active caspase 3 and the cleaved form of Poly (ADP-Ribose) Polymerase (PARP) was observed (Fig. 5a, b).

Increase in protein nitration

The contribution of protein nitration was assessed to further characterize the mechanisms underlying the increase in ROS (H_2O_2 and $O_2^{\bullet}$) contributing to T4-mediated apoptosis. As shown in Fig. 6a, the long-term treatment with T4 increased the levels of protein nitration of tyrosine residues. In addition, we previously showed that PKCζ is an essential enzyme in the signaling pathways leading to BW cell proliferation and is associated with iNOS [25, 27]. To evaluate whether long-term treatment with T4 would lead to PKCζ tyrosine nitration, we immunoprecipitated the PKCζ isoform and assessed the presence of nitrotyrosine residues using a specific antibody. The results suggest that PKCζ is nitrated on tyrosine through oxidant molecules. PKCζ nitration is evident after 5 days of T4 incubation (data not shown), reaching a maximum level after 15 days of HT treatment (Fig. 6b).

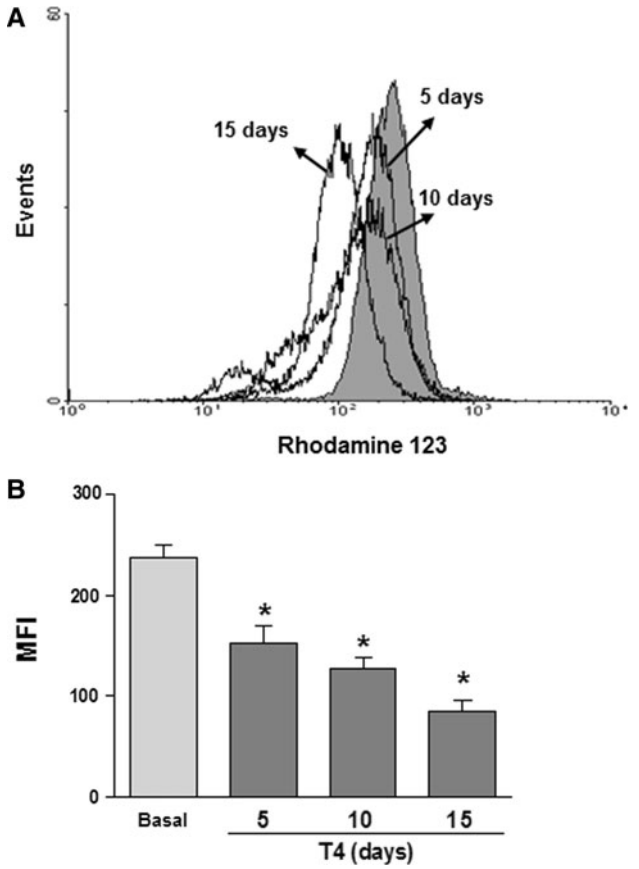

Fig. 4 Mitochondrial participation in the apoptotic process. BW cells were cultured under basal conditions or in the presence of T4 (10^{-7} M) for the indicated times and stained with Rodhamine-123 to assess changes in mitochondrial membrane potential through flow cytometry. **a** The histograms are representatives of 4 independent experiments. **b** The *bar graph* displays the mean fluorescence intensity values (MFI) ± SE. * Differ significantly from the corresponding basal values, with at least $P < 0.01$

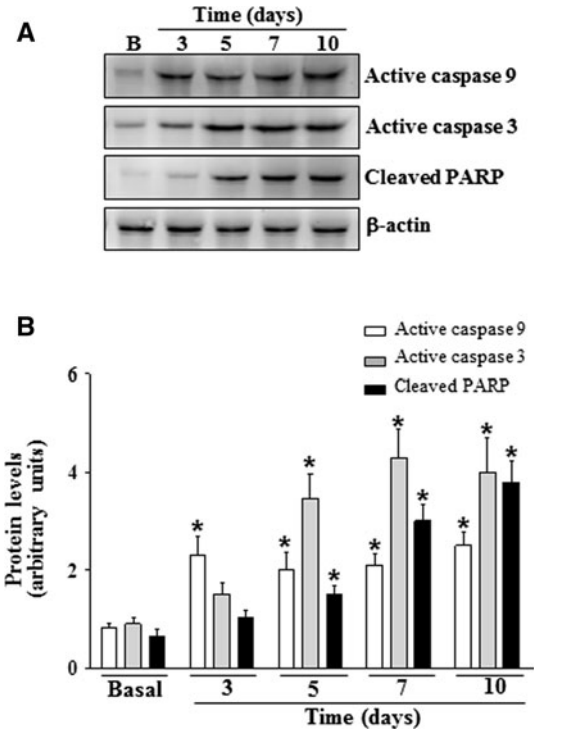

Fig. 5 Proteolytic activation of caspases and Poly (ADP-Ribose) Polymerase (PARP) cleavage. The cells were cultured in the absence (Basal) or the presence of T4 (10^{-7} M) for the indicated times. The proteolytic activation of caspases 9 and 3 and cleavage of PARP were analyzed through western blotting. Specific antibodies showed bands of 37 (active caspase 9), 17 (active caspase 3), 89 (cleaved PARP) and 43 kDa (β-actin). The densitometric results of the western blot analysis are shown in the *bar graphs*. The values represent the mean ± SE of 3 independent experiments. The β-actin bands were used as control for protein loading. * Differ significantly respect to the control, with $P < 0.05$

To determine whether PKCζ nitration auto regulates the expression of this isoform, the PKCζ content was evaluated through western blot analysis in cellular extracts from BW cells treated with T4 for the indicated times. The results showed that long-term treatment with T4 reduced PKCζ protein levels (Fig. 6c). The co-incubation of BW cells with T4 and L-NAME inhibited both nitration (Fig. 6b) and reduction of PKCζ cellular content (Fig. 6d), suggesting that enzyme nitration is a requisite for the reduction in the PKCζ levels. To determine whether the nitration of tyrosine residues facilitates enzyme degradation through the proteasome pathway, the cellular content of PKCζ was determined in the presence of T4 and the proteasome inhibitor MG132. As shown in Fig. 6e, treatment with MG132 inhibited the reduction in the PKC cellular content, suggesting that protein nitration facilitates PKC degradation.

Discussion

Despite the conflicting evidence concerning the role of THs in the induction of apoptosis in immune cells, the results of the present study clearly show that the duration of treatment with THs is crucial for the regulation of cell fate, as T4 triggers a cascade of biochemical events, including protein nitration, responsible for the generation of the apoptotic response. In T lymphoma cells, these events occur after 5 days of culture in the presence of the hormone and follow an initial proliferative response induced through T4 [25–27]. These time-dependent effects were shown through characteristic morphological changes, DNA ladder formation, and Annexin V-FITC/PI co-staining. Notably, T3 induced apoptosis with a kinetic course similar to that of T4. However, increased variations were observed when the cells were treated with T3 and are potentially associated with cross talk between genomic and nongenomic actions that impact the balance between proliferative

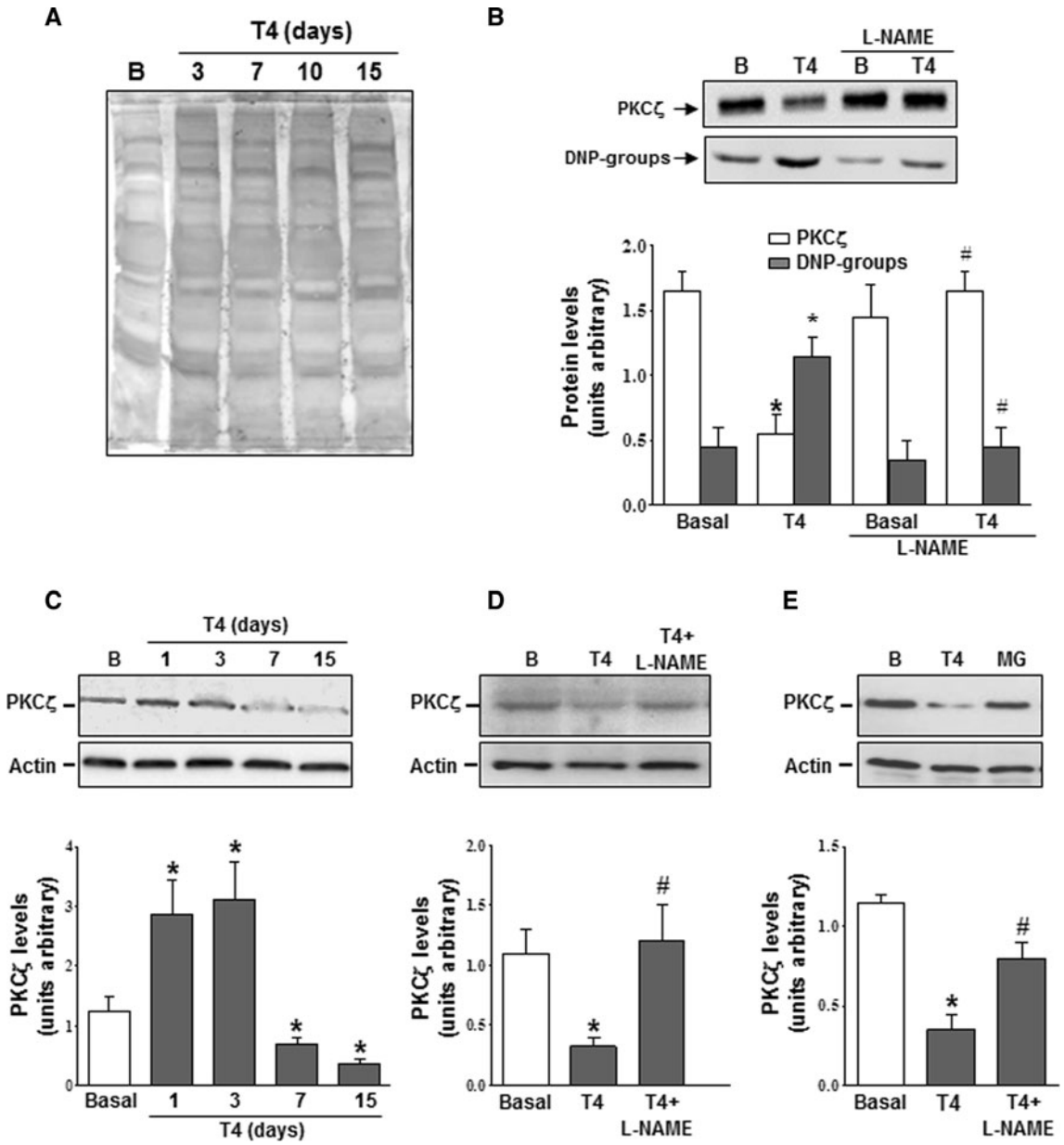

Fig. 6 Protein nitration and PKCζ intracellular levels. **a** BW cells were cultured in the absence (Basal, B) or the presence of T4 (10^{-7} M) for the indicated times and protein nitration was analyzed using an anti-p-tyr antibody through western blot assays. The gel is representative of 4 gels obtained from 2 independent experiments. **b** The anti- PKCζ immunoprecipitation assay on extracts from cells treated or not with T4 in the absence or the presence of L-NAME (200 μM) for 10 days. After immunoprecipitation and SDS-PAGE, the proteins were revealed using an anti-PKCζ antibody (*upper panel*) or an antibody against nitro-tyrosine residues (*lower panel*). The densitometry analysis of the western blot results is shown in the *bar graphs*. The values represent the mean ± SE of 4 independent experiments. **c** The intracellular levels of PKCζ were determined through western blot analysis of the extracts of cells incubated in the absence or presence of T4 for the indicated times. The results are representative of 4 independent experiments. The actin bands were used as control for protein loading. The densitometry analysis of the western blot results is shown in the *bar graphs*. **d** and **e** Effect of NOS and proteasome inhibition on T4-mediated regulation of PKCζ levels. BW cells were cultured with T4 in the presence of the NOS blocker L-NAME (200 μM) (**d**) or the proteasome inhibitor MG132 (100 nM) (**e**) for 10 days. The densitometry analysis of the western blot results is shown in the *bar graphs*. The results are representative of 2 independent experiments. * Significantly different from the corresponding basal values or # the corresponding T4 values, with at least $P < 0.05$

versus cell death induction. In addition, the possibility that the short T3 half-life inhibits the actions of T3 on apoptosis cannot be precluded. Indeed, T4 is the hormone typically used in replacement therapies in hypothyroid patients due to its higher half-life compared with that of T3, facilitating a constant potency and prolonged action, with subsequent

conversion to T3 through deiodinase [33]. Thus, the mechanisms involved in the actions of T4 were further studied. Our results are consistent with those observed in Jurkat lymphoma cell line [28], where both T3 and T4 induce apoptosis after 14 days of culture. In addition, T3 hormone treatment for 5 days enhanced the apoptosis of both CD4+ and CD8+ T lymphocytes purified from human peripheral blood lymphocytes. Shorter incubation times (24 h) were required to induce apoptosis through THs when T cells were obtained from patients with Graves' disease, in which cells are chronically exposed to high levels of circulating THs [28]. Furthermore, long-term treatment with T3 inhibited cell proliferation through the induction of time-dependent apoptosis in a murine osteoblast precursor cell line [34].

The mechanisms accompanying T4-mediated apoptotic events include an increase in the mRNA and protein levels of iNOS, resulting in a marked increase in NOS activity and $^{\bullet}$NO production. Indeed, T4-mediated enhanced $^{\bullet}$NO generation has been demonstrated in tadpole tail apoptosis and is associated with increased oxidative stress [35]. Oxidative stress is mediated through ROS production encompassing a diverse range of species, including superoxide, hydrogen peroxide, nitric oxide, peroxynitrite, hypochlorous acid, singlet oxygen and the hydroxyl radical [36]. Thus, we investigated the role of oxidative species in the T4-mediated apoptosis of BW T cells. To examine the balance of the redox state of the cell and it correlation with the induction of apoptotic mechanisms, both DCFH-DA and HE probes were used to evaluate the levels of intracellular ROS and determine the GSH/GSSG ratio. Although DCFH-DA and HE are not specific for detecting intracellular H_2O_2 and intracellular $O_2^{\bullet -}$, respectively, these probes demonstrate the presence of cellular oxidative stress [37]. We observed an increase in the ROS content and the oxidized form of glutathione at the expense of its reduced form and a decrease in the GSH/GSSG ratio. These results indicate that long-term treatment of BW cells with T4 affects oxidative damage. Increases in ROS stress induce various biological responses, ranging from transient growth arrest and adaptation, increased cellular proliferation, permanent growth arrest or senescence, apoptosis, and necrosis [38]. The precise outcomes are dependent on the cellular genetic background, the types of the specific ROS involved, and the levels and duration of the ROS stress [38]. Indeed, the participation of ROS production in tumor proliferation and resistance to drug-induced death was recently demonstrated in human colon cancer, which is mediated through the ROS-induced transcriptional activation of the NFκB pathway [39]. We demonstrated that 24–48 h of treatment with T4 induces the proliferation of T lymphoma cells, with the involvement of PKCζ and downstream NFκB activation [27]; however, no ROS production was observed (unpublished observations). Thus, the cumulative production of ROS induced through long-term treatment (5 or more days) with T4 might be associated with the altered redox regulation of cellular signaling pathways leading to cell death. The excessive production of ROS might damage various cellular components, including DNA, protein, and lipid membranes [40]. Moreover, the increment in the oxidized form of glutathione at the expense of its reduced form might be associated with sustained ROS stress conditions that might exhaust the redox buffering systems responsible for maintaining the balance between ROS generation and elimination [41]. Indeed, GSH is particularly relevant in cancer cells, as this compound is involved in the regulation of several carcinogenic mechanisms, including DNA synthesis, cell proliferation and death, and also influences cancer cell sensitivity against cytotoxic drugs or ionizing radiation [42]. An increase in oxidative stress, evidenced through the reduced GSH cellular content and GSH/GSSG ratio and increased DCF fluorescence, was observed after the incubation of human lymphoma cells with an antineoplastic drug, thus indicating that this mechanism is involved in cytotoxic drug-induced apoptosis [43]. In addition, the depletion of GSH enhances the induction of apoptosis through a therapeutic agent in lymphoma cells [44]. In addition, oxidative stress induces the intrinsic pathway of apoptosis, resulting in mitochondrial membrane depolarization with a loss of membrane potential. Thus, cytochrome C is released from the mitochondria to the cytosol, triggering the activation of the caspase cascade, which is responsible, along with oxidizing species, for cell death [45]. The long-term culture of BW cells in the presence of T4 showed a significant increase in the loss of mitochondrial membrane potential, the activation of caspases 9 and 3 and the cleavage of PARP. Caspase 3 is a key downstream effector in the apoptosis pathway, amplifying the signal of the initiator caspase 9 and leading to PARP cleavage in lymphocytes in response to several apoptotic stimuli [46]. These results confirm that T4 treatment for more than 5 days leads to a cascade of events, including membrane depolarization and ROS production, culminating in cell apoptosis.

When analyzing the intracellular signaling cascades involved in the long-term effects of T4 on BW cells, we observed an increase in PKCζ levels at 24–72 h after T4 treatment (see also [25]), followed by an abrupt decrease after 5 days of T4 treatment, which was inhibited through co-incubation with the NOS competitive inhibitor L-NAME, thus indicating the involvement of $^{\bullet}$NO in these effects. Most of the cytotoxicity attributed to $^{\bullet}$NO is primarily due to peroxynitrite, the product of the diffusion-controlled reaction of this free radical with the superoxide anion radical. Peroxynitrites are reactive nitrogen species

(RNS) that interact with lipids, DNA, and proteins via direct oxidative reactions or nitration mechanisms, thus triggering cellular responses that culminate in overwhelming oxidative injury, committing cells to necrosis or apoptosis [47]. The potential participation of RNS in the T4-mediated reduction of PKCζ levels was evaluated. We observed an increase in the levels of nitrated proteins and the specific nitration of PKCζ, as demonstrated through immunoprecipitation assays, suggesting that the decrease of PKCζ levels observed after long-term treatment with T4 was most likely associated with tyrosine nitration, as this effect was also inhibited using L-NAME. The nitration of proteins generally accelerates proteasome degradation [48]. Indeed, the proteasome inhibitor MG132 inhibited the T4-mediated reduction of PKCζ. As this enzyme is essential for BW cell division and survival, the reduced intracellular PKCζ levels might contribute to the apoptotic process. According to our results, peroxynitrites are primarily responsible for protein nitration in human leukocytes [49] and are also involved in the nitration and inhibition of PKC isoenzymes, including PKCζ, in hippocampal neurons [50]. Moreover, the overexpression of PKCζ in intestinal cells confers protection against oxidative stress through iNOS [51]. However, the $^{\bullet}$NO-mediated tyrosine nitration of antioxidant enzymes has been described in mouse glial cells, leading to mitochondrial dysfunction and subsequent apoptosis [52]. Indeed, we observed an increase in the total levels of tyrosine-nitrated proteins, suggesting that similar mechanisms might occur in our experimental system. Thus, the nitration of antioxidant enzymes could modulate the cellular redox state and contribute to the induction of cell apoptosis.

The kinetic course of T4-mediated apoptotic events, iNOS levels, $^{\bullet}$NO production and PKCζ degradation requires special discussion. DNA fragmentation is maximal at 15 days, and PKCζ degradation accompanied this event. However, the production of $^{\bullet}$NO is highest after 7 days, with iNOS expression drastically diminishing after 15 days. Notably, the delay in the induction of apoptosis through THs in T lymphoma cells is associated with the fact that short-term treatment with both T3 and T4 induces the proliferation of this cell line [25, 27]. Therefore, this delay in induction is likely associated with the balance between proliferative versus apoptotic signals that become evident after 5 days. Lymphoma BW5147 is a T cell line dependent on both $^{\bullet}$NO and PKCζ activity for proliferative survival [26, 53]. At 24–72 h of incubation with THs induces cell proliferation, NOS and PKCζ activation and increased enzyme mRNA and protein levels in BW cells. [26]. According to our results, the $^{\bullet}$NO and iNOS were maintained after treatment with T4 for 5 days, leading to even higher levels of NOS activity than those observed at 72 h, consequently generating higher levels of $^{\bullet}$NO that would induce the cascade of apoptotic, instead of proliferative, signals. The fact that the NOS values after 15 days were similar to basal levels is difficult to explain, as at this time point, less than 3 % of the cell population is viable according to the Annexin-FITC staining. Cell counting at this time point with Trypan blue exclusion dye showed $\sim 6 \pm 3$ % viable cells (data not shown). Thus, one possible explanation is that high NOS levels in a few cells might compensate for cellular loss, showing values similar to those observed in the untreated cell population. A dual effect was described for $^{\bullet}$NO, depending on its concentration in cancer cells [54], and intracellular events induced through high levels of nitric oxide precedes apoptotic events in pancreatic cells [55]. This cascade might lead to oxidative stress and PKCζ degradation, resulting in cell death. The maximum degradation of PKCζ is also evident after 15 days of T4 treatment, thus indicating that the levels of this enzyme must most likely be reduced for the induction of apoptosis to occur. The atypical PKCζ was demonstrated to play an important role in apoptosis induction in several cell types. Indeed, the ototoxic aminoglycoside antibiotic amikacin induced PKCζ cleavage concomitant with chromatin condensation in the cochlea of amikacin-treated rats [56]. In addition, $^{\bullet}$NO production in primary culture articular chondrocytes induces apoptosis and $^{\bullet}$NO-induced apoptosis requires the down-regulation of PKCζ [57]. Reduced $^{\bullet}$NO production and NOS activity after 15 days is likely associated with the reduced iNOS expression and increased number of apoptotic cells observed at this time.

In conclusion, these results indicate that the long-term treatment of BW cells with T4 leads to iNOS-induced oxidant up-regulation, which reduces protective PKCζ levels through nitration and increased proteasome degradation, culminating in cellular apoptosis.

Moreover, the role of THs on tumor cell growth is controversial. Hypothyroidism differentially affects tumor growth and invasiveness. Martínez-Iglesias et al. [58] showed that hypothyroid mice display smaller, but more invasive, tumors than euthyroid mice. Although the results obtained in the present study are only from in vitro analyses, this evidence might clarify the dual action of THs in tumor growth, as THs induce either T tumor cell division or apoptosis, depending on chronic or acute exposure to hormonal stimulus. While these observations require further studies, these findings suggest a role for THs in modulating T lymphocyte pathophysiology.

Acknowledgments The authors wish to thank Mrs María Rosa Gonzalez Murano for her excellent technical assistance. This work was supported by Grants from the Consejo Nacional de Investigaciones Científicas y Técnicas (CONICET), PIP-CONICET N° 00275, from Agencia Nacional para la Promoción Científica y Técnica, PICT 2008 N° 1858 and from University of Buenos Aires, UBACYT N° 20020100100291.

References

1. Alisi A, Demori I, Spagnuolo S, Pierantozzi E, Fugassa E, Leoni S (2005) Thyroid status affects rat liver regeneration after partial hepatectomy by regulating cell cycle and apoptosis. Cell Physiol Biochem 15:69–76. doi:10.1159/000083639
2. Scapin S, Leoni S, Spagnuolo S, Gnocchi D, De Vito P, Luly P, Pedersen JZ, Incerpi S (2010) Short-term effects of thyroid hormones during development: focus on signal transduction. Steroids 75(8–9):576–584. doi:10.1016/j.steroids.2009.10.013
3. Wang YY, Jiao B, Guo WG, Che HL, Yu ZB (2010) Excessive thyroxine enhances susceptibility to apoptosis and decreases contractility of cardiomyocytes. Mol Cell Endocrinol 320(1–2): 67–75. doi:10.1016/j.mce.2010.01.031
4. Pascual A, Aranda A (2012) Thyroid hormone receptors, cell growth and differentiation. Biochim Biophys Acta. doi:10.1016/j.bbagen.2012.03.012
5. Davis PJ, Leonard JL, Davis FB (2008) Mechanisms of nongenomic actions of thyroid hormone. Front Neuroendocrinol 29:211–218. doi:10.1016/j.yfrne.2007.09.003
6. Ishizuya-Oka A (2011) Amphibian organ remodeling during metamorphosis: insight into thyroid hormone-induced apoptosis. Dev Growth Differ 53(2):202–212. doi:10.1111/j.1440-169X.2010.01222.x
7. Miyata K, Ose K (2012) Thyroid hormone-disrupting effects and the amphibian metamorphosis assay. J Toxicol Pathol 25(1):1–9. doi:10.1293/tox.25.1
8. Contreras-Jurado C, García-Serrano L, Gómez-Ferrería M, Costa C, Paramio JM, Aranda A (2011) The thyroid hormone receptors as modulators of skin proliferation and inflammation. J Biol Chem 286(27):24079–24088. doi:10.1074/jbc.M111.218487
9. Ledda-Columbano GM, Molotzu F, Pibiri M, Cossu C, Perra A, Columbano A (2006) Thyroid hormone induces cyclin D1 nuclear translocation and DNA synthesis in adult rat cardiomyocytes. FASEB J 20(1):87–94. doi:10.1096/fj.05-4202com
10. Ledda-Columbano GM, Perra A, Pibiri M, Molotzu F, Columbano A (2005) Induction of pancreatic acinar cell proliferation by thyroid hormone. J Endocrinol 185(3):393–399. doi:10.1677/joe.1.06110
11. Columbano A, Pibiri M, Deidda M, Cossu C, Scanlan TS, Chiellini G, Muntoni S, Ledda-Columbano GM (2006) The thyroid hormone receptor-beta agonist GC-1 induces cell proliferation in rat liver and pancreas. Endocrinology 147(7):3211–3218. doi:10.1210/en.2005-1561
12. Di Fulvio M, Coleoni AH, Pellizas CG, Masini-Repiso AM (2000) Tri-iodothyronine induces proliferation in cultured bovine thyroid cells: evidence for the involvement of epidermal growth factor-associated tyrosine kinase activity. J Endocrinol 166(1): 173–182. doi:10.1677/joe.0.1660173
13. Bedó G, Pascual A, Aranda A (2011) Early thyroid hormone-induced gene expression changes in N2a-β neuroblastoma cells. J Mol Neurosci 45(2):76–86. doi:10.1007/s12031-010-9389-y
14. Wagner MS, Wajner SM, Maia AL (2008) The role of thyroid hormone in testicular development and function. J Endocrinol 199(3):351–365. doi:10.1677/JOE-08-0218
15. González-Sancho JM, Figueroa A, López-Barahona M, López E, Beug H, Muñoz A (2002) Inhibition of proliferation and expression of T1 and cyclin D1 genes by thyroid hormone in mammary epithelial cells. Mol Carcinog 34(1):25–34. doi:10.1002/mc.10046
16. Yehuda-Shnaidman E, Kalderon B, Bar-Tana J (2005) Modulation of mitochondrial transition pore components by thyroid hormone. Endocrinology 146(5):2462–2472. doi:10.1210/en.2004-1161
17. Chiloeches A, Sánchez-Pacheco A, Gil-Araujo B, Aranda A, Lasa M (2008) Thyroid hormone-mediated activation of the ERK/dual specificity phosphatase 1 pathway augments the apoptosis of GH4C1 cells by down-regulating nuclear factor-kappaB activity. Mol Endocrinol 22(11):2466–2480. doi:10.1210/me.2008-0107
18. Sar P, Peter R, Rath B, Das Mohapatra A, Mishra SK (2011) 3,3′5 Triiodo L-thyronine induces apoptosis in human breast cancer MCF-7 cells, repressing SMP30 expression through negative thyroid response elements. PLoS One 6:e20861. doi:10.1371/journal.pone.0020861
19. Yamada-Okabe T, Satoh Y, Yamada-Okabe H (2003) Thyroid hormone induces the expression of 4-1BB and activation of caspases in a thyroid hormone receptor-dependent manner. Eur J Biochem 270(14):3064–3073. doi:10.1046/j.1432-1033.2003.03686.x
20. Zhang L, Cooper-Kuhn CM, Nannmark U, Blomgren K, Kuhn HG (2010) Stimulatory effects of thyroid hormone on brain angiogenesis in vivo and in vitro. J Cereb Blood Flow Metab 30:323–335. doi:10.1038/jcbfm.2009.216
21. Lin HY, Tang HY, Keating T, Wu YH, Shih A, Hammond D, Sun M, Hercbergs A, Davis FB, Davis PJ (2008) Resveratrol is pro-apoptotic and thyroid hormone is anti-apoptotic in glioma cells: both actions are integrin and ERK mediated. Carcinogenesis 29:62–69. doi:10.1093/carcin/bgm239
22. Balázs C, Leövey A, Szabó M, Bakó G (1980) Stimulating effect of triiodothyronine on cell-mediated immunity. Eur J Clin Pharmacol 17(1):19–23. doi:10.1007/BF00561672
23. Keast D, Taylor K (1982) The effect of tri-iodothyronine on the phytohaemagglutinin response of T lymphocytes. Clin Exp Immunol 47(1):217–220
24. Ong ML, Malkin DG, Malkin A (1986) Alteration of lymphocyte reactivities by thyroid hormones. Int J Immunopharmacol 8(7):755–762. doi:10.1016/0192-0561
25. Barreiro Arcos ML, Gorelik G, Klecha A, Genaro AM, Cremaschi GA (2006) Thyroid hormones increase inducible nitric oxide synthase gene expression downstream from PKC-zeta in murine tumor T lymphocytes. Am J Physiol Cell Physiol 291(2):C327–C336
26. Barreiro Arcos ML, Gorelik G, Klecha A, Goren N, Cerquetti C, Cremaschi GA (2003) Inducible nitric oxide synthase-mediated proliferation of a T lymphoma cell line. Nitric Oxide 8(2): 111–118. doi:10.1016/S1089-8603(02)00181-7
27. Barreiro Arcos ML, Sterle HA, Paulazo MA, Valli E, Klecha AJ, Isse B, Pellizas CG, Farias RN, Cremaschi GA (2011) Cooperative nongenomic and genomic actions on thyroid hormone mediated-modulation of T cell proliferation involve up-regulation of thyroid hormone receptor and inducible nitric oxide synthase expression. J Cell Physiol 226(12):3208–3218. doi:10.1002/jcp.22681
28. Mihara S, Suzuki N, Wakisaka S, Suzuki S, Sekita N, Yamamoto S, Saito N, Hoshino T, Sakane T (1999) Effects of thyroid hormones on apoptotic cell death of human lymphocytes. J Clin Endocrinol Metab 84(4):1378–1385. doi:10.1210/jc.84.4.1378
29. Hodkinson CF, Simpson EE, Beattie JH, O'Connor JM, Campbell DJ, Strain JJ, Wallace JM (2009) Preliminary evidence of immune function modulation by thyroid hormones in healthy men and women aged 55–70 years. J Endocrinol 202(1):55–63. doi:10.1677/JOE-08-0488
30. Hermann M, Lorenz H, Voll R, Grunke M, Woith W, Kalden JR (1994) A rapid and simple method for the isolation of apoptotic DNA fragments. Nucleic Acids Res 22(24):5506–5507. doi:10.1093/nar/22.24.5506
31. Walsh GM, Dewson G, Wardlaw AJ, Levi-Schaffer F, Moqbel R (1998) A comparative study of different methods for the assessment of apoptosis and necrosis in human eosinophils. J Immunol Methods 217(1–2):153–163. doi:10.1016/S0022-1759(98)00103-3
32. Griffith OW (1980) Determination of glutathione and glutathione disulfide using glutathione reductase and 2-vinylpyridine. Anal Biochem 106(1):207–212. doi:10.1016/0003-2697(80)90139-6
33. Ma C, Xie J, Huang X, Wang G, Wang Y, Wang X, Zuo S (2009) Thyroxine alone or thyroxine plus triiodothyronine replacement

therapy for hypothyroidism. Nucl Med Commun 30:586–593. doi:10.1097/MNM.0b013e32832c79e0
34. Fratzl-Zelman N, Hörandner H, Luegmayr E, Varga F, Ellinger A, Erlee MP, Klaushofer K (1997) Effects of triiodothyronine on the morphology of cells and matrix, the localization of alkaline phosphatase, and the frequency of apoptosis in long-term cultures of MC3T3-E1 cells. Bone 20:225–236. doi:10.1016/S8756-3282(96)00367-5
35. Kashiwagi A, Hanada H, Yabuki M, Kanno T, Ishisaka R, Sasaki J, Inoue M, Utsumi K (1999) Thyroxine enhancement and the role of reactive oxygen species in tadpole tail apoptosis. Free Radic Biol Med. 26:1001–1009. doi:10.1016/S0891-5849(98)00296-2
36. Murphy MP, Holmgren A, Larsson NG, Halliwell B, Chang CJ, Kalyanaraman B, Rhee SG, Thornalley PJ, Partridge L, Gems D, Nyström T, Belousov V, Schumacker PT, Winterbourn CC (2011) Unraveling the biological roles of reactive oxygen species. Cell Metab 13(4):361–366. doi:10.1016/j.cmet.2011.03.010
37. Kalyanaraman B, Darley-Usmar V, Davies KJ, Dennery PA, Forman HJ, Grisham MB, Mann GE, Moore K, Roberts LJ, Ischiropoulos H (2012) Measuring reactive oxygen and nitrogen species with fluorescent probes: challenges and limitations. Free Radic Biol Med 52(1):1–6. doi:10.1016/j.freeradbiomed.2011.09.030
38. Pelicano H, Carney D, Huang P (2004) ROS stress in cancer cells and therapeutic implications. Drug Resist Updates 7:97–110. doi:10.1016/j.drup.2004.01.004
39. Formentini L, Sánchez-Aragó M, Sánchez-Cenizo L, Cuezva JM (2012) The mitochondrial ATPase inhibitory factor 1 triggers a ROS-mediated retrograde prosurvival and proliferative response. Mol Cell 45(6):731–742. doi:10.1016/j.molcel.2012.01.008
40. Hensley K, Robinson KA, Gabbita SP, Salsman S, Floyd RA (2000) Reactive oxygen species, cell signaling, and cell injury. Free Radic Biol Med 28:1456–1462. doi:10.1016/S0891-5849(00)00252-5
41. Tarpey MM, Wink DA, Grisham MB (2004) Methods for detection of reactive metabolites of oxygen and nitrogen: in vitro and in vivo considerations. Am J Physiol Regul Integr Comp Physiol 286(3):R431–R444
42. Ortega AL, Mena S, Estrela JM (2011) Glutathione in cancer cell death. Cancers 3:1285–1310. doi:10.3390/cancers3011285
43. Yang M, Chitambar CR (2008) Role of oxidative stress in the induction of metallothionein-2A and heme oxygenase-1 gene expression by the antineoplastic agent gallium nitrate in human lymphoma cells. Free Radical Biol Med 45(6):763–772. doi:10.1016/j.freeradbiomed.2008.05.031
44. Bhalla S, Gordon LI, David K, Prachand S, Singh ATK, Yang S, Winter JN, Guo D, O'Halloran T, Platanias LC, Evens AM (2010) Glutathione depletion enhances arsenic trioxide-induced apoptosis in lymphoma cells through mitochondrial-independent mechanisms. Br J Haematol 150(3):365–369. doi:10.1111/j.1365-2141.2010.08197.x
45. Simon HU, Haj-Yehia A, Levi-Schaffer F (2000) Role of reactive species (ROS) in apoptosis induction. Apoptosis 5(5):415–418. doi:10.1023/A:1009616228304
46. Shao N, Zou J, Li J, Chen F, Dai J, Qu X, Sun X, Ma D, Ji C (2012) Hyper-activation of WNT/β-catenin signaling pathway mediates anti-tumor effects of histone deacetylase inhibitors in acute T lymphoblastic leukemia. Leuk Lymphoma 53(9):1769–1778. doi:10.3109/10428194.2012.663085
47. Pacher P, Beckman JS, Liaudet L (2007) Nitric oxide and peroxynitrite in health and disease. Physiol Rev 87(1):315–424
48. Souza JM, Choi I, Chen Q, Weisse M, Daikhin E, Yudkoff M, Obin M, Ara J, Horwitz J, Ischiropoulos H (2000) Proteolytic degradation of tyrosine nitrated proteins. Arch Biochem Biophys 380(2):360–366. doi:10.1006/abbi.2000.1940
49. Galiñanes M, Matata BM (2002) Protein nitration is predominantly mediated by a peroxynitrite-dependent pathway in cultured human leucocytes. Biochem J 367(Pt 2):467–473. doi:10.1042/BJ20020825
50. Knapp LT, Kanterewicz BI, Hayes EL, Klann E (2001) Peroxynitrite-induced tyrosine nitration and inhibition of protein kinase C. Biochem Biophys Res Commun 286(4):764–770. doi:10.1006/bbrc.2001.5448
51. Banan A, Zhang L, Fields JZ, Farhadi A, Talmage DA, Keshavarzian A (2002) PKC-zeta prevents oxidant-induced iNOS upregulation and protects the microtubules and gut barrier integrity. Am J Physiol Gastrointest Liver Physiol 283(4):G909–G922
52. Tangpong J, Sompol P, Vore M, St Clair W, Butterfield DA, St Clair DK (2008) Tumor necrosis factor alpha-mediated nitric oxide production enhances manganese superoxide dismutase nitration and mitochondrial dysfunction in primary neurons: an insight into the role of glial cells. Neuroscience 151(2):622–629. doi:10.1016/j.neuroscience.2007.10.046
53. Gorelik G, Barreiro Arcos ML, Klecha AJ, Cremaschi GA (2002) Differential expression of protein kinase C isoenzymes related to high nitric oxide synthase activity in a T lymphoma cell line. Biochim Biophys Acta 1588:179–188. doi:10.1016/S0925-4439(02)00163-1
54. Burke AJ, Sullivan FJ, Giles FJ, Glynn SA (2013) The yin and yang of nitric oxide in cancer progression. Carcinogenesis 34:503–512. doi:10.1093/carcin/bgt034
55. Cahuana GM, Tejedo JR, Jimenez J, Ramırez R, Sobrino F, Bedoya FJ (2004) Nitric oxide-induced carbonylation of Bcl-2, GAPDH and ANT precedes apoptotic events in insulin-secreting RINm5F cells. Exp Cell Res 293:22–30. doi:10.1016/j.yexcr.2003.10.004
56. Lecain E, Omri B, Behar-Cohen F, Tran Ba Huy P, Crisanti P (2007) The role of PKCzeta in amikacin-induced apoptosis in the cochlea: prevention by aspirin. Apoptosis 12:333–342. doi:10.1007/s10495-006-0580-0
57. Kim JS, Park ZY, Yoo YJ, Yu SS, Chun JS (2005) p38 kinase mediates nitric oxide-induced apoptosis of chondrocytes through the inhibition of protein kinase C zeta by blocking autophosphorylation. Cell Death Differ 12:201–212. doi:10.1038/sj.cdd.4401511
58. Martínez-Iglesias O, García-Silva S, Regadera J, Aranda A (2009) Hypothyroidism enhances tumor invasiveness and metastasis development. PLoS One 4(7):e6428. doi:10.1371/journal.pone.0006428